Predictability of North Atlantic Multidecadal Climate Variability

Stephen M. Griffies* and Kirk Bryan

Atmospheric weather systems become unpredictable beyond a few weeks, but climate variations can be predictable over much longer periods because of the coupling of the ocean and atmosphere. With the use of a global coupled ocean-atmosphere model, it is shown that the North Atlantic may have climatic predictability on the order of a decade or longer. These results suggest that variations of the dominant multidecadal sea surface temperature patterns in the North Atlantic, which have been associated with changes in climate over Eurasia, can be predicted if an adequate and sustainable system for monitoring the Atlantic Ocean exists.

Historical data for sea surface temperatures (SSTs) indicate that the North Atlantic has experienced significant multidecadal climate variability superimposed on a positive trend (*1*, *2*). It has been shown (*3*) that a yearly to decadal time scale propagation of SST anomalies may be traced in the surface circulation around the North Atlantic subpolar gyre. Pioneering work by Talley and McCarthy (*4*) has indicated the existence of decadal changes in the lower thermocline from flow originating in the Labrador Sea, and the large-scale multidecadal changes that have taken place in the Atlantic sea level have been documented (*5*). These studies, especially that of Hansen and Bezdek (*3*), indicate that the variability in mid-depth to surface Atlantic Ocean properties contains a significant amount of coherence over multiple years to decades, thus suggesting that nontrivial predictability of such climatic fluctuations may be possible. It is a primary objective of several climate research programs to assess the possibilities for projecting climate over decadal and longer time scales (*6*, *7*). For this purpose, it is essential to quantify the predictability of such variability as it manifests itself in the ocean because the ocean represents the source of memory on which useful long-term climate forecasts could be based.

Here we present a study directed at quantifying the predictability time scales for North Atlantic and high-latitude multidecadal variability. It was necessary to use a numerical model because the predictability cannot be established from the available historical record. A coupled ocean-atmosphere model was used to reduce the uncertainties related to boundary conditions introduced with ocean models forced by highly simplified atmospheric parameterizations (*8*). Also, a realistic atmospheric component is essential because climate predict-

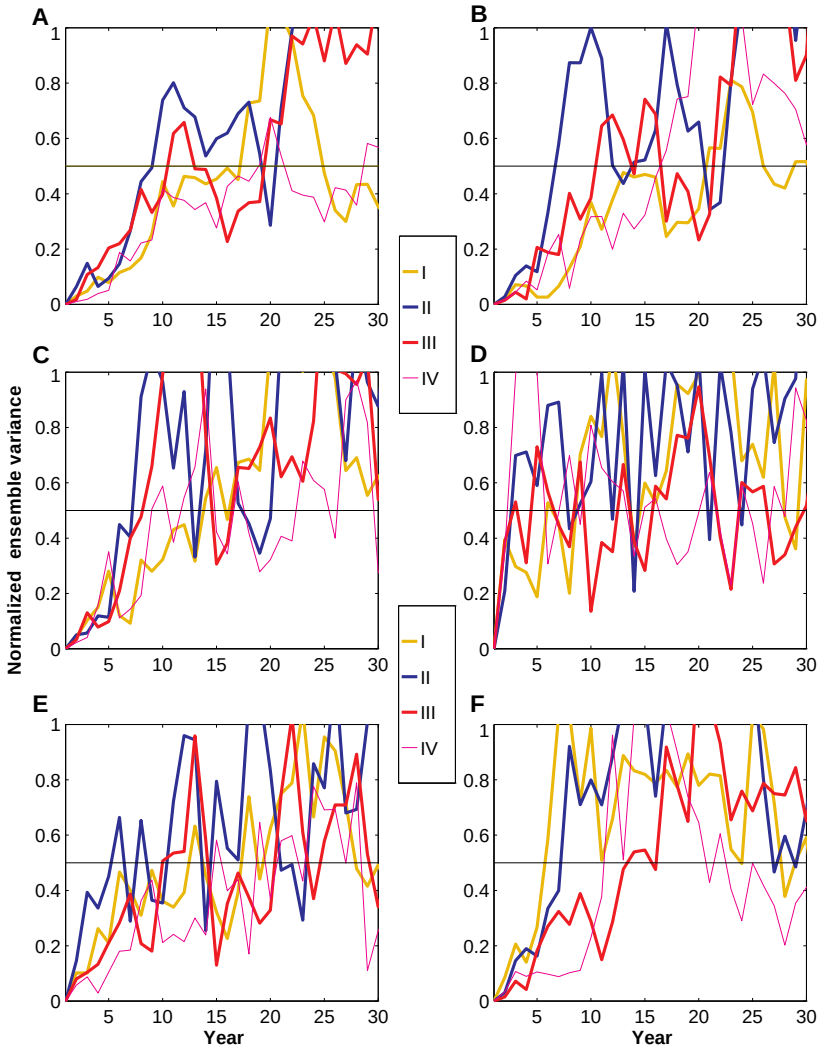

Fig. 1. Normalized ensemble variances for selected principal component time series as a function of time from the four ensembles of simulations. Ensemble I contains 12 members and was initialized with the ocean at year 130 from the control simulation (*12*), and the linear detrended climatology from years 1 to 200 was used for defining its associated climatology patterns and statistics. Ensemble II has 12 members, was initialized with the ocean at year 500, and used climatology from years 401 to 600. Ensembles III and IV have eight members, each were initialized with the ocean at years 941 and 951, respectively, and used climatology from years 801 to 1000. The full 1000-year simulation (*12*) contains a nonlinear drift, which motivated our choice for 200-year climatologies, each of which showed only a modest linear drift. Presented here are results for the North Atlantic (0° to 70°N latitude and 0° to 90°W longitude) (**A**) first EOF (EOF1) for dynamic topography, (**B**) EOF1 for temperature at a depth of 170 m (this field is indicative of the very clean subsurface signals associated with the multidecadal variability), (**C**) SSS EOF1, (**D**) SST EOF1, (**E**) EOF2 for the meridional streamfunction of the zonally integrated Atlantic (50°S to 90°N latitude) velocity (streamfunction EOF1 represents a basin-wide drift and is not of interest here), and (**F**) SST averaged over 15° to 25°W at 70°N in the East Greenland Sea. The ensembles used to generate these statistics represent 1200 years of integration from the coupled model.

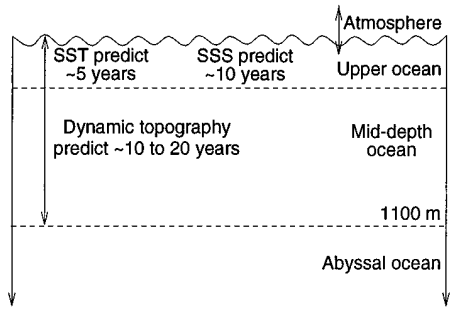

Fig. 2. Schematic diagram of the oceanic predictability seen in the coupled model. The surface ocean serves as the interface between the noisy synoptic atmosphere and the more coherent mid-depth ocean. When the mid-depth ocean properties are oscillating, the surface properties and those at mid-depth contain multiyear to multidecadal predictability. The oscillation is seen most distinctly in the dynamic topography.

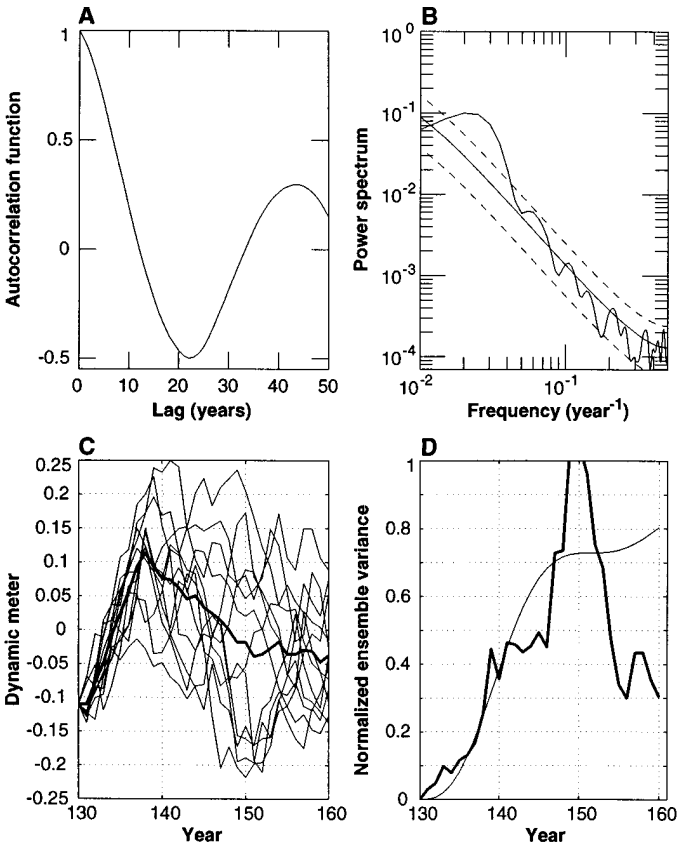

Fig. 3. (**A**) Autocorrelation function for the first North Atlantic dynamic topography's first principal component defined from yearly mean fields for model years 1 to 200. The abscissa is the lag in years. The time series were linearly detrended before computation of the eigenfunctions (EOF patterns) of the zero-lag covariance matrix. The damped sine-wave behavior is characteristic of oscillatory variability. This sample autocorrelation function can be fitted to that from a damped harmonic oscillator driven by white noise, where the oscillator period and damping time are ~40 years each. (**B**) Power spectrum corresponding to the previous autocorrelation function. The power rises well above the 95% red noise null hypothesis bounds (the dashed lines) in the 40- to 60-year time scale. (**C**) The principal-component trajectories from the ensemble I simulation for dynamic topography EOF1. The dark solid line indicates the ensemble mean. (**D**) The normalized ensemble variance for the trajectories in (C), with the thin smooth line being the variance predicted from an infinite-sized ensemble of the noise-driven damped harmonic oscillator.

ability cannot be estimated properly without taking into account the effectively random fluctuations of synoptic atmospheric forcing (*9, 10*). To quantify predictability, we integrated the coupled model many times starting from atmospheric conditions chosen randomly from the model's climatology, but with identical oceanic initial conditions. We constructed four such ensembles (designated I, II, III, and IV) of simulations to assess the sensitivity of the model's multidecadal variability to the initial atmospheric state.

The coupled model we used was developed at the Geophysical Fluid Dynamics Laboratory (GFDL) to study climate (*11*). Of interest is the model's multidecadal variability seen in a 1000-year control simulation (*12, 13*). The strongest multidecadal signals from the control simulation are those located in the mid-latitude to subpolar Atlantic regions associated with variations in the thermohaline circulation (THC) (*12*), as well as variability in the high-latitude Greenland Sea region (*13*). For the North Atlantic THC variability, there is a strong association between fluctuations in the oceanic overturning and changes in the thermocline density distribution and sea surface properties. The high-latitude Greenland Sea variability is associated with the propagation of freshwater anomalies southward from the Arctic within the East Greenland current into the North Atlantic (*13*). The model signals from these events strongly influence the SSTs east of central Greenland.

To partition climate variability into dominant spatiotemporal patterns, it is useful to construct empirical orthogonal functions (EOFs). For many geophysical phenomena, the dominant EOF patterns have both the largest space and longest time scales. We focused on the dominant EOFs because they also approximate those patterns of greatest predictability. The amplitude of an EOF pattern defines its principal component time series. The principal component time series for the different elements of an ensemble are initially nearly coincident in phase space. The rate at which the phase space trajectories spread over time quantifies the pattern's sensitivity to the randomly chosen atmospheric initial conditions. A useful measure of the spread is the variance, or mean-square difference from the ensemble mean. This statistic, normalized by the variance contained in the climatology, was calculated for various dominant patterns in the model for the four ensembles of simulations (Fig. 1). The time at which the ensemble variance reaches 50% of the climatological variance defines a predictability time for the patterns (Fig. 2) (*14*).

The model's North Atlantic variability is seen quite clearly in the dynamic topography (Fig. 1A), which is the ocean's analog of the pressure surfaces seen on atmospheric weather maps. Dynamic topography is basically the sea surface height taken with respect to a reference level (1100 m was used), and it represents a summary of the ocean's large-scale circulation over the middle to upper ocean. Highly coherent oscillations are exhibited by the dynamic topography over the course of years 1 to 200 from the climatology (Fig. 3).

This damped oscillatory variability can be interpreted within the framework of a simplified paradigm (*15*), on the basis of the idealized meridional-depth THC box model of Stommel (*16*), which describes the ocean circulation changes that could give rise to this form of multidecadal variability in the North Atlantic. In this model, thermohaline overturning is driven by latitudinal buoyancy gradients set up by surface fluxes of heat and salinity. In addition to a time-mean tendency to increase density in northern North Atlantic waters, these fluxes have a large stochastic component associated with synoptic atmospheric disturbances, thus driving the North Atlantic

S. M. Griffies, Geophysical Fluid Dynamics Laboratory, Route 1, Forrestal Campus, Princeton, NJ 08542, USA. E-mail: smg@gfdl.gov
K. Bryan, Princeton University, Atmospheric and Oceanic Sciences Program, Sayre Hall, Forrestal Campus, Princeton, NJ 08544–0710, USA. E-mail: kbryan@splash.princeton.edu
*To whom correspondence should be addressed.

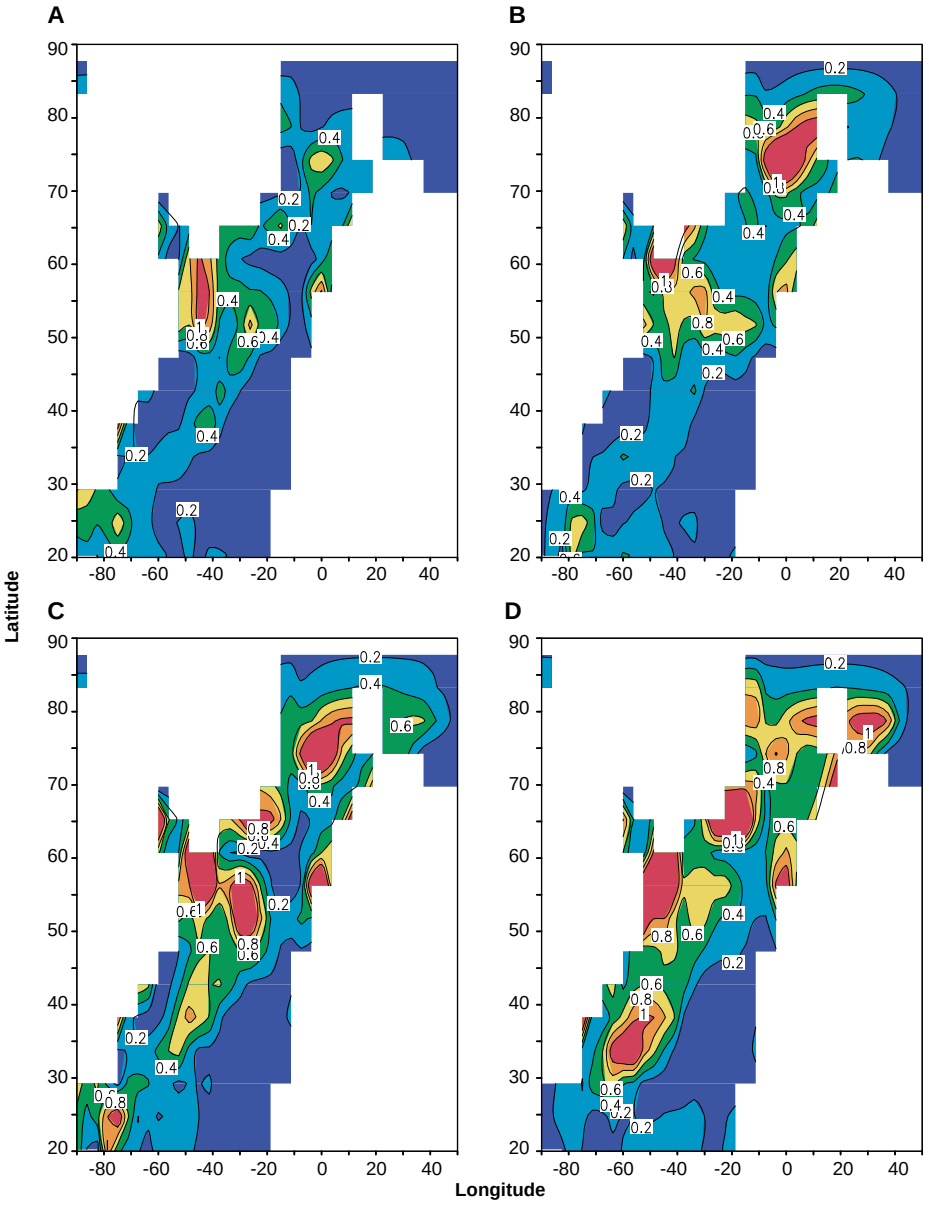

Fig. 4. Maps of the normalized ensemble variance for ensemble I's North Atlantic dynamic topography shown for years 3 (**A**), 5 (**B**), 7 (**C**), and 9 (**D**). The white regions represent land regions. The red regions indicate regions of saturated ensemble variance, and hence rapid loss of predictability. The regions of large variance in years 3 and 5 are associated with areas of strong ocean convection. The subsequent maps illustrate the transfer of this variance southward along the western boundary as well as eastward across the North Atlantic drift. Once convection has initiated a strong growth in ensemble variance, oceanic dynamics act to propagate these errors southward, through the East Greenland current and into the mid-latitudes with a tendency to trap the errors along the western boundary because of the latitudinal variation of the Coriolis force (β effect), except in regions of strong eastward flow such as the northeast regions of the North Atlantic current.

THC on all time scales. The ocean responds to this forcing on the multidecadal time scales, which appear to be the periods preferred by its internal dynamics. Lags in the system enable the ocean circulation to oscillate (*17*).

The results for the ensemble I simulation quantify the predictability time scales realizable when the model's North Atlantic undergoes a nontrivial amount of oscillatory THC variability. In general, the dominant patterns for variables that measure subsurface features, such as dynamic topography, have increased predictability compared with features more directly coupled to atmospheric variability (Fig. 1). Dynamic topography or sea surface height is readily measured through either in situ or remote methods, and thus the high degree of predictability seen for this field suggests that ocean monitoring on a sufficient spatio-temporal scale could be the basis for performing North Atlantic Ocean climate predictions on a 10- to 20-year time scale. Given the success of the current TOPEX/POSEIDON satellite altimeter mission (*18*), we suggest that altimeters could serve as the foundations for a climate monitoring and prediction system. In addition to dynamic topography, we note that sea surface salinity (SSS) is more predictable than SST because SST is more strongly coupled to the atmosphere, thus rendering its anomalies more damped and hence containing a shorter memory. The predictabilities for SST and SSS are lower than for dynamic topography, yet their time scales are much longer in absolute terms than the time scales for other climate signals such as the Tropical Pacific's El Niño–Southern Oscillation (ENSO) (*19*).

The results for the ensemble II simulation quantify predictability when the North Atlantic oscillation is highly damped. The reduction of the variability's oscillatory component implies that predictability depends predominantly on the damped persistence properties of the Hasselmann red noise model (*17*), which provides much less predictability relative to oscillatory dynamics.

Ensembles III and IV have decadal predictability time scales, much as is seen with ensemble I. These latter two ensembles coincide with an extreme negative THC event (more than three standard deviations from the mean) associated with a large freshwater anomaly advecting southward in the East Greenland current. Ensemble III was initialized a few years before the anomaly's effects showed up in the North Atlantic THC, whereas ensemble IV was initialized at the extreme phase of the fluctuation. The ensemble statistics from this event cannot be expected to maintain the simple linear oscillator scaling seen in ensemble I, nor the red noise behavior of ensemble II. The results indicate that if either the large high-latitude freshwater anomaly (ensemble III) or the extreme negative phase (ensemble IV) are initialized in a coupled dynamical model, its effects are predictable for up to two decades in the North Atlantic water mass properties. Additionally, the signal greatly enhances the predictability of the oceanic surface fields.

The multidecadal variability associated with the Greenland Sea oscillation exhibits greater predictability (>5 years) for ensembles I and II than the North Atlantic SST. Associated with the strong freshwater anomaly propagating southward in the Greenland Sea, the Greenland Sea SSTs for ensembles III and IV show predictability for 10 to 15 years. This high predictability could prove to be very important for predicting atmospheric variability because this SST signal has a more significant influence on the model's atmospheric variability over

the high latitudes and parts of Eurasia (*13*) than the North Atlantic SST patterns (*12*).

The spatial structure of the breakdown of predictability can be assessed through a series of ensemble variance maps. Maps taken every other year for ensemble I's ensemble variance for North Atlantic dynamic topography (Fig. 4) show that ensemble variance is initially large in the region directly south of Greenland. Soon thereafter, large values are observed off the coast of east Greenland, which subsequently spread into the northern and northwestern part of the Atlantic. Analysis of convection reveals that the regions of early variance growth are also regions associated with the model's deep water formation. Convection acts as a downward pathway for atmospheric signals. The atmospheric signals were initialized differently for each member of the ensemble, and therefore it may be speculated that convection can enhance the rate of variance growth.

Our results suggest that the basis for long-term North Atlantic climate predictions rests on three physical properties of the North Atlantic Ocean. First, the ocean integrates the mostly "noisy" atmospheric fluxes, thus producing a red power spectrum for oceanic properties on time scales substantially longer than those of the synoptic atmosphere (*17*). This integrative property provides a long-term memory for the coupled ocean-atmosphere system and can be exploited for damped persistence predictions (*20*). Second, there is the special feature of the North Atlantic variability that involves the very active participation of thermohaline dynamics that can provide a significant oscillatory component to the multidecadal variability. These damped, roughly linear, oscillations in the oceanic circulation increase the amplitude of water mass changes at low frequencies over what can be expected from a purely red noise process. The signal from this oscillation can potentially be exploited for making useful multiyear to multidecadal oceanic predictions. Third, strong variations at high latitudes near Greenland are seen in SST, which can influence atmospheric variability extending in a predominantly downstream direction (eastward) (*13*). These variations can also be associated with extreme events in the North Atlantic variability, which are themselves quite predictable. In general, we conjecture that oceanic predictability of the North Atlantic and high-latitude multidecadal variability is greater (reaching up to 10 to 20 years) when the variability has a larger amplitude, including more extreme events.

REFERENCES AND NOTES

1. M. E. Mann and J. Park, *J. Geophys. Res.* **99**, 25819 (1994).
2. C. K. Folland, T. N. Palmer, D. E. Parker, *Nature* **320**, 602 (1986).
3. D. V. Hansen and H. F. Bezdek, *J. Geophys. Res.* **101**, 8749 (1996).
4. L. D. Talley and M. S. McCarthy, *J. Phys. Oceanogr.* **12**, 1189 (1982).
5. S. Levitus, *J. Geophys. Res.* **95**, 5233 (1990).
6. A. L. Gordon, S. E. Zebiak, K. Bryan, *Eos* **73**, 161 (1992).
7. CLIVAR Science Plan, World Climate Research Program, no. 89 (1995).
8. A. J. Weaver and T. M. C. Hughes, *Trends Phys. Oceanogr.* **1**, 15 (1992).
9. E. N. Lorenz, *Tellus* **17**, 321 (1965).
10. T. Palmer, in *NATO Advanced Study Institute: Decadal Climate Variability: Dynamics and Predictability,* D. Anderson and J. Willebrand, Eds. (Springer, Berlin, 1996), pp. 83–156.
11. S. Manabe, R. J. Stouffer, M. Spelman, K. Bryan, *J. Clim.* **4**, 785 (1991).
12. T. Delworth, S. Manabe, R. J. Stouffer, *ibid*. **6**, 1993 (1993).
13. ———, *Geophys. Res. Lett*., in press.
14. With an *F*-test, the differences between ensemble variances and the climatological variance are significant at the 95% level only for ensemble variances less than 50% of the climatological variance.
15. S. M. Griffies and E. Tziperman, *J. Clim.* **8**, 2440 (1995).
16. H. Stommel, *Tellus* **13**, 224 (1961).
17. This oscillator paradigm should be contrasted to the purely damped model of K. Hasselmann [*ibid.* **18**, 473 (1976)], which results in a red noise power spectrum. The essential element contributing to the oscillatory behavior is the thermohaline circulation, which provides an added dynamical mechanism for an oscillation that is absent in the Hasselmann model.
18. L.-L. Fu and R. D. Smith, *Bull. Am. Meteorol. Soc.* **77**, 2625 (1996).
19. D. J. Neelin, M. Latif, and F.-F. Jin [*Annu. Rev. Fluid Mech.* **26**, 617 (1994)] indicate that ENSO has a perfect model predictability on the order of 1 to 2 years.
20. E. Lorenz, *J. Appl. Meteorol.* **12**, 543 (1973).

21. We thank J. Anderson, J. Mahlman, S. Manabe, and E. Tziperman for useful suggestions and R. J. Stouffer and T. Delworth for their assistance in carrying out the ensemble calculations and sharing the results of the GFDL climate model's control experiment. Funding for S.M.G. was provided by a fellowship from the NOAA Postdoctoral Program in Climate and Global Change and NOAA's Geophysical Fluid Dynamics Laboratory. Support for S.M.G. and K.B. was also provided by Atlantic Climate Change Program funding from NOAA's Office of Global Change.

23 September 1996; accepted 19 November 1996

The Origin of Gravitational Lensing: A Postscript to Einstein's 1936 *Science* Paper

Jürgen Renn, Tilman Sauer, John Stachel

Gravitational lensing, now taken as an important astrophysical consequence of the general theory of relativity, was found even before this theory was formulated but was discarded as a speculative idea without any chance of empirical confirmation. Reconstruction of some of Einstein's research notes dating back to 1912 reveals that he explored the possibility of gravitational lensing 3 years before completing his general theory of relativity. On the basis of preliminary insights into this theory, Einstein had already derived the basic features of the lensing effect. When he finally published the very same results 24 years later, it was only in response to prodding by an amateur scientist.

Sixty years ago, Einstein published a short note in *Science* entitled "Lens-Like Action of a Star by the Deviation of Light in the Gravitational Field" (*1*). The note is often considered as the pioneering study of gravitational lensing, although earlier contributions have been recognized [(*2*), chap. 1]. In 1920, Eddington discussed the possibility of seeing multiple images of a star if a massive object, acting as a gravitational lens, is suitably interposed between the star and an observer (*3*). A few years later, Chwolson pointed out that if a star, lens, and observer are in alignment, the observer will see a ring-shaped image of the star centered on the lens (*4*). Einstein's paper of 1936 deals with both effects in apparent ignorance (*5*) of these publications but is free of some of their shortcomings. However, it only gives the final formulas without any derivations. In view of this historical account and Chwolson's pioneering work, it has been suggested (*6*) that the ring-shaped images be renamed "Chwolson rings" rather than the current "Einstein rings."

In the course of a research project on the genesis of general relativity at the Max Planck Institute for the History of Science, we have identified and reconstructed calculations by Einstein on gravitational lensing closely related to his 1936 paper in notes dated to the spring of 1912. These notes show that Einstein had developed the basic theory of gravitational lensing even before he completed the general theory of relativity in 1915.

Exploring consequences of a heuristic assumption about static gravitational fields, Einstein in 1911 published a paper on the deflection of light by the gravitational field of the sun (*7*). The prediction of light bending was confirmed in 1919 by the famous solar eclipse expedition led by Eddington.

J. Renn and T. Sauer, Max Planck Institute for the History of Science, Wilhelmstrasse 44, D-10117 Berlin, Germany.
J. Stachel, Department of Physics, Boston University, Boston, MA 02215, USA.